Check for updates

Article

Urban Analytics and City Science

EPB: Urban Analytics and City Science
2023, Vol. 50(4) 1023–1038
© The Author(s) 2022
Article reuse guidelines:
sagepub.com/journals-permissions
DOI: 10.1177/23998083221131572
journals.sagepub.com/home/epb
Sage

Estimating the effects of urban green regions in terms of diffusion

Eric K Tokuda, Henrique F de Arruda, Guilherme S Domingues and Luciano da F Costa
São Carlos Institute of Physics, University of São Paulo, Brazil

Florence AS Shibata and Roberto M Cesar-Jr
Institute of Mathematics and Statistics, University of São Paulo, Brazil

Cesar H Comin
Department of Computer Science, Federal University of São Carlos, Brazil

Abstract

The interaction between cities and their respective green regions corresponds to an interesting issue that has received growing attention over the last decades. These relationships have multiple natures, ranging from providing habitat for animal life to temperature and humidity dynamics. Several methods based on area, size, shape, and distance have been considered in the literature. Given that several important contributions of green regions to urban areas involve temperature, humidity, and gases exchanges, which are intrinsically related to physical diffusion, it becomes particularly interesting to simulate the diffusion of green effects over urban areas as a means of better understanding the respective influences. The present work reports a related approach. Once the green regions of a given city are automatically identified by semantic segmentation and have eventual artifacts eliminated, successive convolutions are applied as a means to obtain the unfolding of the diffusion of the green effects along time. As illustrated, the diffusion dynamics is intrinsically interesting because it can be strongly affected by the spatial distribution of the green mass. In particular, we observed that smaller green regions could substantially contribute to the diffusion. The reported approach has been illustrated with respect to the Brazilian city of Ribeirão Preto, whose small- and medium-sized green regions were found to complement in an effective manner the diffusion of the green effects as inferred from the performed simulations under specific parameter settings.

Keywords

green space, urban simulation, complexity sciences, network graphs

Corresponding author:
Eric K Tokuda, São Carlos Institute of Physics, University of São Paulo, Rua do matao, 1010, São Carlos 05508-900, Brazil.
Email: tokuda.ek@gmail.com

Introduction

As we progress into the 21st century, important issues remain as a subject of scientific research, including the study of the quality of life in cities and towns, which is not only a multidisciplinary problem, but also involves many characteristics and dimensions including but not being limited to mobility, security, and access to common resources such as parks, hospitals, etc. (Zanjirani Farahani et al., 2010). Among these several aspects, the presence of green areas, their distribution, access, effects, etc., have constituted the subject of continuous studies and discussions (Cetin, 2015; Fahrig, 2020; Ovaskainen, 2002; Rusche et al., 2019). Green areas are important in an urban environment for several reasons, including (i) preservation of living species; (ii) attenuation of urban noise; (iii) landscape design; and (iv) leisure. Therefore, it becomes important to devise means for quantifying these effects and interactions in an objective manner, so that different city organizations can be respectively studied and characterized.

Possible quantitative approaches to studying the effect of green regions in urban areas include the consideration of distance from urban spots to the nearest green regions (Rusche et al., 2019), the distribution of the area (Cetin, 2015), size (Antonela et al., 2014), shape (Zhang et al., 2009), and distance between green regions (Santiago and Pascual-Hortal, 2007). Those studies are intrinsically related to the single large or several small (SLOSS) problem (Fahrig, 2020; Ovaskainen, 2002). Though each of these methods are interesting and important in themselves, each of them focuses on a relatively specific property of the studied problem, so that a more complete characterization, modeling and understanding of the presence of green areas in cities should benefit from additional, complementary approaches.

The problem of modeling the diffusion of particles in the air, in particular of gases, has been widely studied in the literature (Earl and Edward, 1973; Lugg, 1968). Several of these works take into other variables, such as the city traffic (Johnson et al., 1973) and the urban morphology (Adolphe, 2001; Jiang et al., 2021). For instance, in (Adolphe, 2001), the authors propose a set of topological and geometrical measurements from the city that can be used, for instance, to study the diffusion of temperature.

The main purpose of the present work is to develop a framework for quantifying the potential effects of green regions in urban areas by taking into account the physical phenomenon of *diffusion*. Indeed, several fundamental dynamics in the physical world are directly related and influenced by diffusion, including thermal propagation, dissemination of gases, as well as the diffusion of elements in water and other liquids. At the same time, several non-linear dynamics often incorporate a diffusive component. Therefore, it becomes interesting to consider the effect of green areas into an urban environment in terms of numerically simulated diffusion of gases, temperature (Maimaitiyiming et al., 2014), humidity, as well as other elements to and from the green areas. In order to isolate the effect of greenery, we carefully considered the morphology of the respective areas. This constitutes the main objective of the present work.

The proposed methodology is applied as follows. Satellite images are systematically collected from a city of interest. A sample of the images are manually annotated regarding the green regions and a deep-learning-based model is trained to automatically identify green regions in the images. Eventual artifacts generated in the segmentation are removed in a post-processing step. The resulting image can then be used as input for the simulation of the diffusion of green effects, which we henceforth call *green diffusion*. The green regions are used as sources and the diffusion is calculated by successive convolutions with a gaussian kernel. We simulate the green regions role as sources by performing a diffusion with sources, that is, at each step, the green areas are replenished to full capacity.

In order to illustrate the potential of the reported methodology, we took into account a satellite image of the city of Ribeirão Preto, Brazil. Having identified the respective green regions, we also

considered two respective versions without the small- and medium-sized green regions, therefore allowing the study of the effect of those areas into the overall obtained diffusion of green effects. Among the several effects that could have been considered, here we focus on humidity diffusion, which corresponds to a potentially important contribution to be derived from the green regions of a city. Interestingly, it was observed that the incorporation of relatively small green areas can substantially boost the diffusion of humidity from the green regions.

This article starts by briefly revising some of the main related works, and proceeds by describing the adopted dataset and segmentation of the respective images regarding their green regions, as well as pre-processing required for removing some segmentation artifacts. The numerical simulation of the diffusion of effects from the green regions is then described. A case example with respect to the a Brazilian city is then presented and discussed.

Related work

Satellite images are employed in various studies and can reveal valuable information about given regions (Bonthoux et al., 2019; He et al., 2020; Tong et al., 2018). One example consists of a study that analyzed the reforestation in China regarding the amount of green vegetation cover along time (Tong et al., 2018). Researchers have also investigated the preferences of people regarding different approaches to implementing green areas in cities (Bonthoux et al., 2019). Another important aspect that has been studied is the impact of temperature changes on vegetation (Herbert and Wurzel, 2003). Furthermore, in another study (He et al., 2020), the authors shows that economic growth can positively impact the green area level, but vegetation development does not necessarily imply economic growth. Researchers also studied the possible relationship between vegetation areas and people's education and income (Nesbitt et al., 2019). The spatiotemporal changes of these green regions, focusing in a particular ecosystem, such as in mountains, is also the topic of several studies, such as in (Bian et al., 2020).

Many distinct aspects, intrinsically related to the interplay between cities' green and urban areas, have been explored (Antonela et al., 2014; Janhäll, 2015; Jin et al., 2018; Robitu et al., 2006). Some of these studies reveal characteristics regarding the influence of vegetation in cities, such as the impact on temperature (Antonela et al., 2014) and carbon storage (Yin et al., 2011). The information regarding rural areas surrounding the city has also been considered (Cui et al., 2019). Interestingly, in (Antonela et al., 2014) the effect of the sizes of the green regions patches on urban heat islands is studied. However, not only the size of the green area plays an essential role in mitigating the effect of the heat islands, but also their pattern (including the border geometry and specific vegetation aspects) (Ren et al., 2015). The authors of (Ali et al., 2015) investigated how urban land surface temperature varies according to diverse patterns of green cover patches. Interestingly, they found that homogeneously dispersed green patches tend to be more efficient in reducing the surrounding area's temperature. The emergence of heat islands motivates researchers to also consider the *distribution* of these green patches (Du et al., 2017; Lin et al., 2015). For instance, in (Lin et al., 2015) the authors estimate the cooling effect of adjacent parks in the city. Moreover, the shape of the green patches can also play an important role in the land surface temperature (Zhang et al., 2009). Although many studies have described the importance and impact of vegetation in cities, the authors of (Xing and Peter, 2019) suggest that the greenery of urban parks could play a limited role in air purification.

Other studies deal with model simulations that incorporate characteristics of the real systems (Robitu et al., 2006; Takebayashi, 2017). For example, in (Robitu et al., 2006) the authors deal with the problem of the influence of vegetation and water on the city microclimate by considering computational fluid dynamics. Another simulation approach, proposed in (Takebayashi, 2017), considered the air temperature on the relationship between urban and green areas.

Material and methods

The main steps of the methodology are as follows: (i) dataset acquisition; (ii) segmentation of green areas; (iii) post-processing using mathematical morphology; and (iv) simulation of a diffusion dynamics using the identified green areas as source. These steps, which are illustrated in Figure 1, are explained below.

Dataset acquisition

The images used in this study were obtained from Mapbox (Mapbox, 2010), which provides high-resolution images from many different places. The boundary of the region of interest (i.e., urban area of the cities) was manually identified. Due to the tileset convention (OpenStreetMap, 2018) used in Mapbox API, it is necessary to convert latitudes and longitudes into another set of numerical coordinates before requesting the download of satellite images of the area through the API. In this convention, the entire region is divided into square images with the same sizes (tiles). Each column in this division is mapped to a Y value and each row to a X value. This pair X, Y uniquely identifies a square of the region and covers an interval of coordinates. Providing the list of X, Y coordinates that forms the region, it is possible to retrieve the image of the entire area of interest. Specific technical details of the adopted dataset in our experiments are presented in Section Results and Discussion.

A ground truth dataset was manually generated using the online annotator tool Supervisely (Supervisely, 2018). A sample of the images was randomly inspected (preferably not at the urban periphery) and polygons covering the class of interest (green areas) were generated. As a result, a binary mask for each image is generated indicating the presence of green.

Image segmentation of green areas

To characterize a satellite image, it is usually necessary to first identify its main relevant structures. We start this process by green areas segmentation. Many works have approached the problem of segmenting areas of interest in remote sensing images. For instance, (Barbieri et al., 2011) considered several types of aerial images and, by using the concept of Shannon entropy (Thomas, 1999), sought to distinguish the regions as being urban, rural, or aquatic. More recently, deep-learning methodologies have been considered (Flood et al., 2019; Ivanovsky et al., 2019; Khan et al., 2017; Siti et al., 2016), such as in (Siti et al., 2016), where a CNN (Convolutional Neural Network) was adopted for automatically identifying natural disasters from satellite images. In

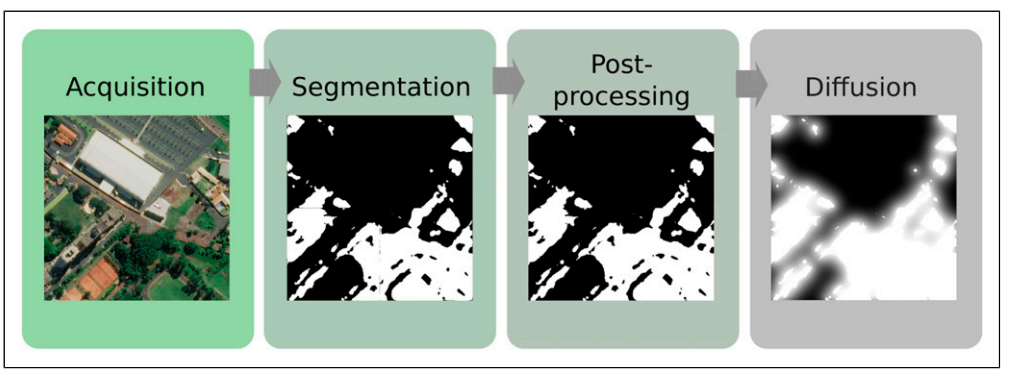

Figure 1. Workflow of the methodology described in the present work.

another study, by using a CNN architecture and temporal information, changes in forest regions have been identified (Khan et al., 2017).

A deep-learning configuration frequently considered in remote sensing studies is the U-Net (Ronneberger et al., 2015), which is also based on convolution layers. More information regarding this architecture is presented in Section 3.2. Interestingly, though the U-Net was originally considered for dealing with biomedical image segmentation (Ronneberger et al., 2015), many studies employed U-Net variations in the analysis of satellite imagery, such as in the detection of buildings (Ivanovsky et al., 2019) and green areas (Flood et al., 2019).

In this study, we focus on inferring the composition of *green areas* in the urban scenery in satellite images, which do not necessarily have a homogeneously green color. Thus, the segmentation of such areas constitutes a challenging task. Here, we consider mostly urban vegetation with green coloration in the definition of Green area: the presence of trees, gardens, squares, yards, flower beds, recreational space with a grass field, trees at roadsides, sidewalks, or between residences. In some cases, plantations near the city borders were included. However, there are some areas for which it is difficult to determine the presence or absence of vegetation, such as plantation harvest regions, muddy or barren regions, and dry grass with yellow coloration. For these ambiguous regions, we take into consideration the presence of trees as a crucial factor to determine if the area were to be considered as a green area or not. In general rules, the presence of trees will indicate the presence of green. As an example, in the Figure 2 there are brown regions surrounded by grass. In Figure 2(a) we can observe the presence of small trees between the region without grass, and thus, this region was labeled as a green area. In contrast, the region shown in Figure 2(b) also has a brown region but without the presence of any tree and thus was not considered as a green area.

After the construction of the supervised dataset, the data is provided to a supervised learning method to identify the green area regions. The model training process for a segmentation task is challenging because it requires predicting the category of each pixel in the image. In this study, a U-Net (Ronneberger et al., 2015) architecture was adopted. The model's architecture is fully convolutional and consists of symmetrical contraction and expansion paths.

Post-processing using mathematical morphology

Because the images are obtained initially as a set of squares, and we employ a tiled-based processing method before assembling the entire image, some artifacts can be respectively implied in the

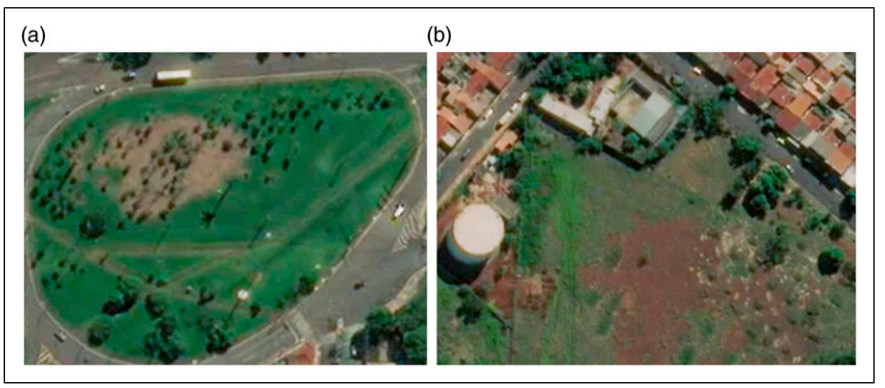

Figure 2. Example of how ambiguous regions are treated: (a) when trees are present in bare soil, the respective region is considered as a green area; (b) bare soil region devoid of trees is not considered a green area.

predicted labels. In general, unwanted vertical and horizontal lines result near the square borders. To deal with this problem, we employed a data-based noise reduction post-processing step. First, we apply morphological closing operation using a disk structuring element to reduce noise. Furthermore, morphological closing is also adopted to remove straight line artifacts. More specifically, this step was constrained to the regions composed of pixels that are no further than six pixels from the tile boundaries. In order to remove both the horizontal and vertical unwanted lines, we processed these regions separately, as four rectangles with an overlap at the four corners. These rectangles are named Left (L), Right ®, Up (U), and down (D), according to their positions. With respect to each of the rectangles, kernels with dimensions 6 × 6 are defined, as follows:

$$\begin{aligned} K_L &= \begin{bmatrix} 0 & 0 & 1 & 1 & 1 & 1 \\ 0 & 0 & 1 & 1 & 1 & 1 \\ 0 & 0 & 1 & 1 & 1 & 1 \\ 0 & 0 & 1 & 1 & 1 & 1 \\ 0 & 0 & 1 & 1 & 1 & 1 \end{bmatrix}, K_R = \begin{bmatrix} 1 & 1 & 1 & 1 & 0 & 0 \\ 1 & 1 & 1 & 1 & 0 & 0 \\ 1 & 1 & 1 & 1 & 0 & 0 \\ 1 & 1 & 1 & 1 & 0 & 0 \\ 1 & 1 & 1 & 1 & 0 & 0 \end{bmatrix}, \\ K_U &= \begin{bmatrix} 0 & 0 & 0 & 0 & 0 & 0 \\ 0 & 0 & 0 & 0 & 0 & 0 \\ 1 & 1 & 1 & 1 & 1 & 1 \\ 1 & 1 & 1 & 1 & 1 & 1 \\ 1 & 1 & 1 & 1 & 1 & 1 \end{bmatrix}, K_D = \begin{bmatrix} 1 & 1 & 1 & 1 & 1 & 1 \\ 1 & 1 & 1 & 1 & 1 & 1 \\ 1 & 1 & 1 & 1 & 1 & 1 \\ 0 & 0 & 0 & 0 & 0 & 0 \\ 0 & 0 & 0 & 0 & 0 & 0 \end{bmatrix}. \end{aligned} \tag{1}$$

By considering each of these kernels, we compute their convolutions with the respective rectangles. To obtain regions with the same size as the original rectangle, the convolution is performed with zero-padding. The resultant matrix is formed by real numbers. So, to convert this matrix to binary numbers, a threshold, τ, is applied, and the values above τ are converted to 1, otherwise being assigned 0 (here, we use $\tau = 0.5$). This operation starts from the rectangle L, and the remaining are computed by following the order: R, U, and D. Note that, for the overlapped regions, this operation is performed twice so as to remove both the horizontal and vertical artifacts.

Green diffusion

Nature and vegetation are essential in promoting healthy living on earth. Thus, it becomes important to analyze the distribution of the green and non-green regions in its cities.

The diffusion is the displacement of an element (e.g., energy, water molecules) from a region to another, generally occurring from the higher concentration region to the lower concentration one (Crank, 1979). There are several mathematical approaches to modeling diffusion, and they are commonly categorized between normal and anomalous diffusion, depending whether the process obeys the Fick's law or not (Fick, 1855). In the specific case of diffusion of particles in the air, turbulent diffusion (Egan and James, 1972; Majda and Kramer, 1999; Roberts and Webster, 2002; Warhaft, 2000) is often considered, which is governed by

$$\frac{\partial c}{\partial t} + \mathbf{u}\nabla c = D\nabla^2 c \tag{2}$$

where c, varying along position and time, represents the concentration of the substance, D is the diffusion coefficient, which in this case is assumed constant in space and time, and u represents a turbulent flow (also varying along time and space), which takes into account the atmospheric forces (Garratt, 1994). In this case, u may dominate the equation, in which case it leads to an anomalous diffusion process. A simplification of this approach ignores the atmospheric effects, reducing it to the normal diffusion equation:

$$\frac{\partial c}{\partial t} = D\nabla^2 c \tag{3}$$

Here, we propose a physics-inspired approach for characterizing the interaction between co-existing green and non-green regions, which we call *green diffusion*. A simple process characterizing several natural phenomena is as a two-dimensional normal and isotropic diffusion, or simply diffusion (Crank, 1979) which, for simplicity's sake, is henceforth considered in the present work. For instance, the diffusion of humidity follows this type of dynamics. This provides one of the main motivations for the present work, namely, the simulation of a diffusion process emanating from the green regions into the non-green areas. If allowed to unfold along time, defining a respective signature, such a diffusion dynamics can provide an indication about the potential influence of the green regions over the other areas. The specific profile observed in these signatures can vary largely depending not only on the proximity, but also on the *geometry* of the green regions. Several desired green effects such as humidity, soil preservation, air filtering—not to mention providing habitat for birds and small animals—which contribute to environmental and urbanistic aspects, can be reasonably modeled in terms of a linear diffusive dynamics. The green regions are represented as corresponding to sources of diffusion. More specifically, their values are kept constant at all times.

We model the diffusion of the humidity in terms of point source isotropic diffusion (Arfken and Weber, 1999), approached in terms of a two-dimensional point-spread function $P(r, t)$ by using the following equation:

$$P(r,t) = \frac{e^{-\left(\frac{r^2}{4Dt}\right)}}{4\pi Dt} \tag{4}$$

where r is the distance (in m) to the source, t (in s) corresponds to the time, and D is the diffusion coefficient (in m^2/s).

In a more practical aspect, this method can be computed through successive convolutions with the green region (Arfken and Weber, 1999). First, a mask with value one representing the green areas, and zero otherwise, is created by considering the green areas segmented from the satellite image. For each iteration, the image is convolved with a smooth kernel (e.g., Gaussian). This procedure is repeated n times, to simulate the diffusion of humidity throughout the city.

As an alternative dynamics, we consider the diffusion with sources. This approach starts with the same process employed in the former methodology. However, at the end of each iteration, the intensity of the initially detected green regions is set to one again. Here, the number of iterations is controlled by the following equation:

$$c = \frac{\text{area}_{\text{green}}}{\text{area}_{\text{total}}}, \tag{5}$$

where $\text{area}_{\text{green}}$ is the number of pixels reached by the green diffusion, and $\text{area}_{\text{total}}$ is the total number of pixels in the image. The dynamics finish when $t \leq c$, where t is a parameter. An interesting measure, obtained from these simulations, is the time required to achieve a desired overall green level.

Interestingly, though corresponding to a ubiquitous phenomenon in nature, diffusion dynamics can vary in surprising manners depending on the spatial distribution and size of the green sources. This important issue is illustrated in Figure 3, which depicts three distinct distributions of green regions but with the same total green area. The three considered types of green spatial distributions can be summarized as follows: (a) a single, large connected area, for instance, as corresponding to parks and squares; (b) a branched distribution of vegetation, as typically observed around rivers and streams; and (c) a large number of relatively small vegetation areas, as in gardens and backyards, distributed in a nearly uniform manner. Also shown in Figure 3 are waterfall diagrams containing the histograms of the diffused green effect along time, given by the concentration of pixels respectively to each of the three considered configurations.

The first important result is that quite distinct green diffusion profiles can be obtained with respect to each of the three types of spatial distribution. The case involving a single, large green area led to histograms indicating large frequency of relatively low diffused effects, therefore corresponding to a little effective influence of the green region as gauged by diffusion. The branched case yielded a relatively more effective diffusion, with histograms being shifted to the right. However, the third type of green spatial distribution, involving a relatively uniform spreading of small vegetation areas, resulted in the most effective diffusion of humidity from the city green regions, being substantially distinct from the other two types of distribution types. This result is particularly important with respect to the present work because: (i) it shows that the diffusion can critically and abruptly vary in non-intuitive manner depending on the size and spatial spread of the green areas and (ii) the most effective diffusion of a total green area takes place for several small regions distributed in nearly uniform manner.

Results and discussion

Dataset and implementation details

To illustrate the proposed methodology, we select a Brazilian city, Ribeirão Preto. Our methodology starts by acquiring satellite images, identifying green areas, and analyzing a dynamical process considering this topology. The satellite images used in this study were obtained using the Mapbox Raster Tiles API (Mapbox, 2010), with the zoom at level 18, which corresponds to the resolution of approximately 0.6 m/pixel, providing high-resolution images from the entire region of the city. With this resolution, a total of 49,911 tile images were acquired to compose the entire region of the city. The three-band RGB color images, with size 512 × 512 each, were obtained in the year 2018.

A total of 150 images were annotated and mapped into binary labels. Applying rotations of 90, 180, and 270° to augment available data for model training, a total of 600 images were used and then divided into training, validation and test sets with 70%, 20%, and 10% split proportions, respectively.

The model was implemented in Python using Keras and TensorFlow libraries. The Adam optimizer was used in the network training with a learning rate 0.00,015 and the dice coefficient loss function. The number of epochs was set to 100 and the mean dice coefficient reached 95% on the test dataset. Here, we applied a threshold of 0.6 to consider a pixel as belonging to a green area. The segmentation experiments were carried out in a GeForce GTX 1080 Ti graphics card. Training the neural network took approximately 3 h in this hardware.

An example of segmentation of the green regions in the satellite image of Ribeirão Preto (Figure 4(a)) according to the adopted methodology (Section 3.2) is shown in white in Figure 4(b). Rural areas were removed using a mask (Figure 4(c)) that is applied to the segmentation result, yielding the result shown in Figure 4(d). This mask was obtained by manual segmentation of the estimated urban region.

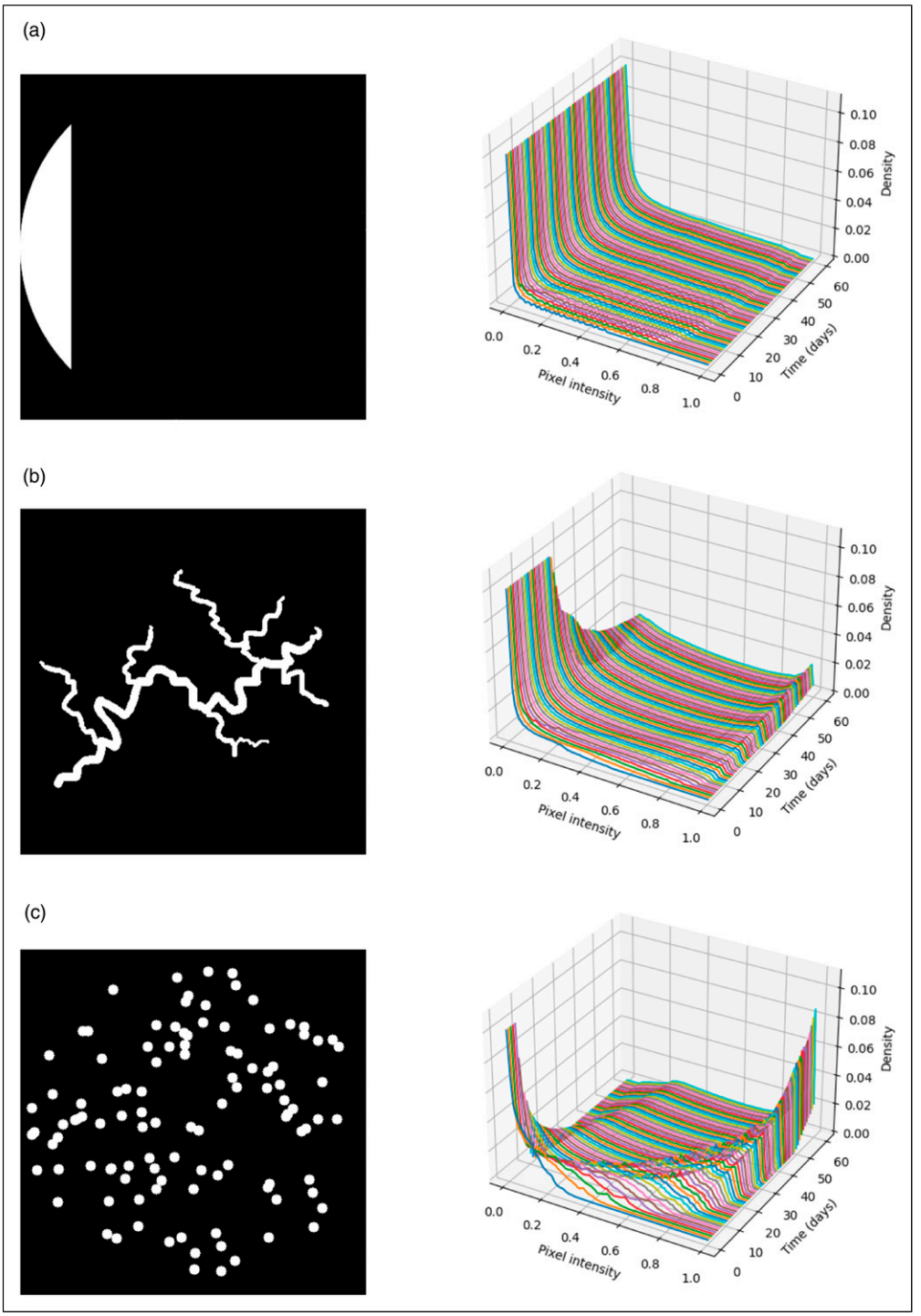

Figure 3. Diffusion with sources for three toy models (a), (b), and (c). The first column shows different green area distributions and the second column shows the corresponding histograms across time. Observe the different scales in the histograms density axes, for the sake of better visualization.

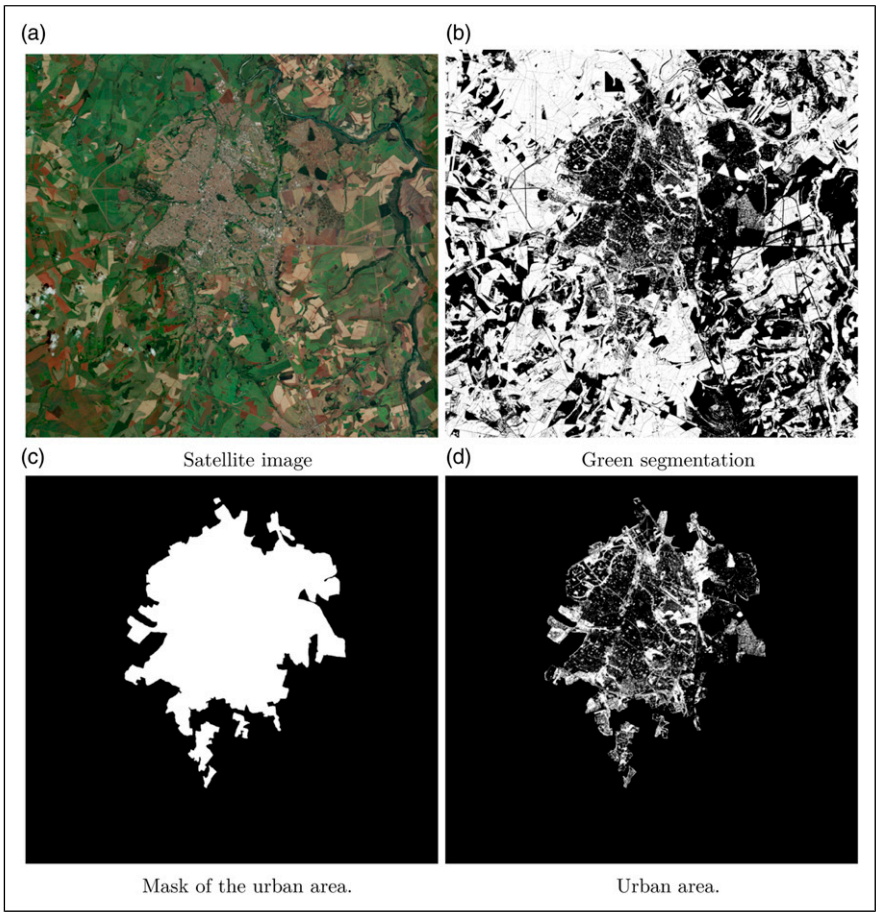

Figure 4. Satellite image (a) and corresponding segmentation of green areas (b) from the city of Ribeirão Preto. Satellite image obtained from Mapbox© (Mapbox, 2010). In order to remove the rural areas, a mask (c) is applied to the segmentation result in (b), yielding (d).

Diffusion of the green effects

The obtained masks were downsampled by 8× the original image, resulting in a frame of size 7360 × 6944. The adopted convolution mask was a square 201-pixel sides window with values determined by equation (4). The diffusion coefficient of the water was adopted as $D = 2.6 \times 10^{-5}\ m^2/s$ (Wang, 1965). Pixels lying outside of the image are considered as having value of zero (free boundary condition). All measurements were handled in the S.I., including the distances in the image (1 pixel = 0.19 m) The process was evaluated for 100 steps.

In order to study the effect of the green region area on the overall diffusion, we consider not only all the identified green area, shown in Figure 5(a), but also two additional images obtained by removing the green regions with area smaller than or equal to $5A$, where $A = 100$ is the typical size of a tree and by removing medium-sized green regions with area smaller than or equal to $2B$, where $B = 1000$ is the typical size of a block. However, given that the removal of the small- and medium-sized green regions effectively reduces the overall green area in those images, it would not be proper to compare the diffusion effects between them. In order to ensure identical overall green areas in the three compared images, we dilated the two thresholded images until they all had the same area as the

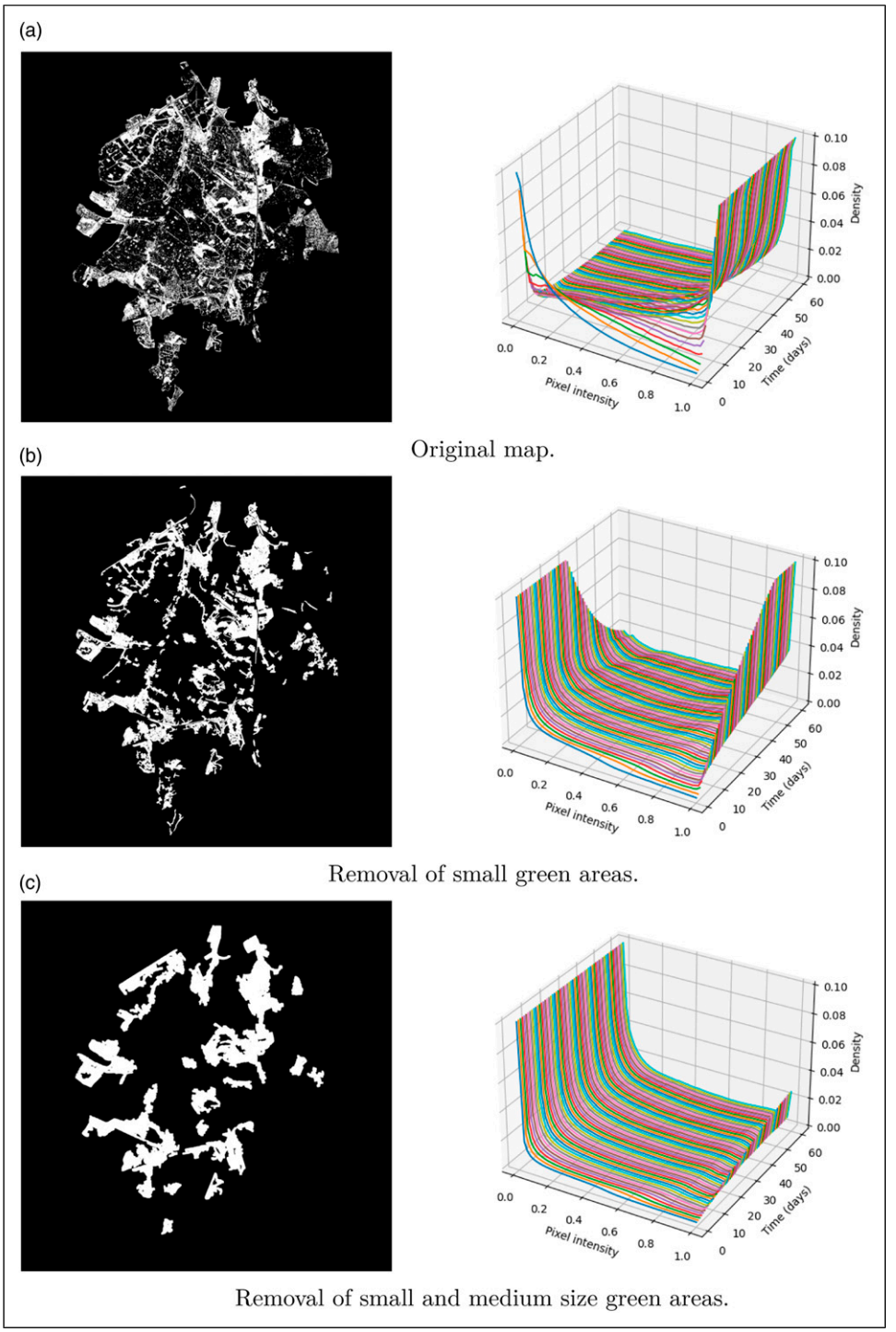

Figure 5. Diffusion of humidity from green sources considering the city of Ribeirão Preto. The first column the originally detected green regions (a), as well as the two considered dilated respective versions of the previous image after removal of small (b) and medium (c) size green areas. The second column contains the corresponding distribution of green along time in the green diffusion.

original image in Figure 5(a). These dilated images are depicted in 5(a) and 5(b), respectively, to the removal of small- and medium-sized green regions.

Figure 5 presents the green diffusion results obtained for (i) the full resolution image of green regions; (ii) the same region after removing connected components smaller than or equal to $5A$; and (iii) the region in (i) after removing all connected component smaller than or equal to $2B$. The consideration of these three situations allows the verification of the effect of the smaller regions on the overall diffusion dynamics.

The results obtained in all the three considered situations confirm the effect of diffusion of the green effects, in particular humidity, verified in the progressive right-shift of the mass of the histograms in the waterfall plots along time. However, in case (i) the diffusion takes place at a much faster rate, reaching saturation after about 20 diffusion steps. Contrariwise, the situation in (iii) is completely different, with rather slow right-shifting of the mass in the histograms. Situation (ii) represents an intermediate result, but with saturation being observed only after 40 diffusion steps.

These results are in full agreement with our previous experiments in Section 3.4, corroborating further the particularly important effect of the spatial distribution of the green areas on the velocity in which the green effects diffusion can take place. From a real-world perspective, these results suggest that smaller patches of vegetation may play an important role as far as diffusion of green effects as modeled in the present work are concerned.

Conclusions

A good deal of the influence of green regions in an urban environment take place through diffusion (e.g., temperature variations, gases displacement, as well as air humidity), it becomes interesting to simulate the diffusion of these effects from green regions in segmented areas of cities.

The present work reported a related approach, focusing on diffusion of humidity. First, satellite images have their green regions identified and treated as sources of diffusion. Then, diffusion is simulated by using a numerical approach, more specifically successive convolutions with a gaussian kernel. After the diffusion has become nearly stable, histograms of the respectively achieved concentrations at each of the considered pixels are obtained. These histograms provide a particularly effective means for gauging the diffusion of green effects given particular regions and cities of interest.

One particularly interesting question implied by diffusion dynamics concerns the fact that distinct spatial distributions of the green sources, as well as their specific morphology, can have unpredictable and even surprising effects. This has been illustrated with respect to three hypothetical images containing the same total green area distributed as a single compact area, a branched structure remindful of rivers and streams, as well as an almost uniform distribution of small patches of green regions. Interestingly, the histograms of green effects obtained in each of these three cases are markedly distinct, with the latter configuration accounting for the most effective diffusion.

As a real-world case example illustrating the proposed methodology, we took into account the Brazilian city of Ribeirão Preto. In order to study the effect of the size of the green regions, we thresholded the respectively obtained green regions so as to remove the small- and medium-sized areas, while special care (dilation of the threshold images) is applied in order that all the three compared configurations have the same total green area. The respectively obtained simulation results, considering humidity diffusion, suggest that the incorporation of small- and medium-sized green regions could have a significant effect in boosting the diffusion of green effects as far as humidity is concerned, and under the assumed hypothesis (normal and isotropic diffusion). Although it is know that more distributed, smaller regions can contributed to more effective diffusion, the consideration of a real-world city and the specific aspect of humidity diffusion allowed more objective, quantitative results to be obtained that showed that even substantially small regions can

contribute significantly to enhance the diffusion of water vapor. For instance, it was verified that the diffusion was particularly effective when all regions were considered, with the humidity density increasing steadily along the first 10 days. The removal of the small green areas influenced strongly the resulting density, taking almost 2 months for reaching increasing by about 10%. The further removal of the medium size green areas had an even greater impact on the humidity diffusion, with a rather slow increase along months.

It should be kept in mind that the obtained results are respective to the dynamics of diffusion as simulated numerically considering specifically adopted city and parameter configurations in simplified settings (e.g., absence of wind and other external influences, adopted diffusion coefficient, etc.), so that the obtained results correspond only to a rough and specific estimation and significantly different results can be obtained in other situtations. In addition, it should be observed that the considered diffusion dynamics is more closely related only to some of the various important roles of green regions in urban areas. These diverse dynamics present other characteristics not modeled by diffusion, such as the need for larger green areas required for animal life, etc. Additional research is required for validating and extending the reported results with respect to more realistic and diverse configurations.

The methodology and results described in the present work pave the way to several interesting subsequent related studies. For instance, it would be interesting to compare the diffusion dynamics with other types of physical dissemination, such as progressive dilation of regions as observed when expanding or reducing the areas of parks. Another interesting possibility regards the incorporation of effects caused by external effects, such as wind. It would also be interesting to enhance the segmentation methodology so as to be able to distinguish between different types of green regions (e.g., trees, lawns, and bushes), as well as their respective conditions (e.g., dry or wet seasons).

Acknowledgments

We are also grateful to Conselho Nacional de Pesquisa (CNPq) and CAPES.

Declaration of conflicting interests

The author(s) declared no potential conflicts of interest with respect to the research, authorship, and/or publication of this article.

Funding

The author(s) disclosed receipt of the following financial support for the research, authorship, and/or publication of this article: This work was supported by the Eric K. Tokuda thanks FAPESP for sponsorship (grant #2019/01077-3). Henrique F. de Arruda acknowledges FAPESP for sponsorship (grant # 2018/10489-0). Cesar H. Comin thanks FAPESP (grant no. 18/09125-4) for financial support. Luciano da F. Costa thanks CNPq (grant # 307085/2018-0). This work received financial support of the Sao Paulo Research Foundation (FAPESP) grant #2015/22308-2.

References

Adolphe L (2001) A simplified model of urban morphology: application to an analysis of the environmental performance of cities. *Environment and Planning B: Planning and Design* 28(2): 183–200.

Ali A, Bahman JA and Sakieh Y (2015) Assessing the effect of green cover spatial patterns on urban land surface temperature using landscape metrics approach. *Urban Ecosystems* 18(1): 209–222.

Antonela G, Leonardo P, Agustina M, et al. (2014) Size matters: vegetation patch size and surface temperature relationship in foothills cities of northwestern argentina. *Urban Ecosystems* 17(4): 1161–1174.

Arfken GB and Weber HJ (1999) Mathematical methods for physicists.

Barbieri AL, De Arruda GF, Rodrigues FA, et al. (2011) An entropy-based approach to automatic image segmentation of satellite images. *Physica A: Statistical Mechanics and Its Applications* 390(3): 512–518.

Bian J, Li A, Lei G, et al. (2020) Global high-resolution mountain green cover index mapping based on landsat images and google earth engine. *ISPRS Journal of Photogrammetry and Remote Sensing* 162: 63–76.

Bonthoux S, Chollet S, Balat I, et al. (2019) Improving nature experience in cities: what are people's preferences for vegetated streets? *Journal of Environmental Management* 230: 335–344.

Cetin M (2015) Using gis analysis to assess urban green space in terms of accessibility: case study in kutahya. *International Journal of Sustainable Development & World Ecology* 22(5): 420–424.

Crank J (1979) *The Mathematics of Diffusion*. Oxford, UK: Oxford University Press.

Cui Y, Xiao X, Russell BD, et al. (2019) The relationships between urban-rural temperature difference and vegetation in eight cities of the great plains. *Frontiers of Earth Science* 13(2): 290–302.

Du H, Cai W, Xu Y, et al. (2017) Quantifying the cool island effects of urban green spaces using remote sensing data. *Urban Forestry & Urban Greening* 27: 24–31.

Earl WM and Edward AM (1973) *Mobility and Diffusion of Ions in Gases*.

Egan BA and James MR (1972) Numerical modeling of advection and diffusion of urban area source pollutants. *Journal of Applied Meteorology and Climatology* 11(2): 312–322.

Fahrig L (2020) Why do several small patches hold more species than few large patches? *Global Ecology and Biogeography* 29(4): 615–628.

Fick A (1855) Ueber diffusion. *Annalen der Physik* 170(1): 59–86.

Flood N, Watson F and Collett L (2019) Using a u-net convolutional neural network to map woody vegetation extent from high resolution satellite imagery across Queensland, Australia. *International Journal of Applied Earth Observation and Geoinformation* 82: 101897.

Garratt JR (1994) The atmospheric boundary layer. *Earth-Science Reviews* 37(1–2): 89–134.

He Z, Xiao L, Guo Q, et al. (2020) Evidence of causality between economic growth and vegetation dynamics and implications for sustainability policy in Chinese cities. *Journal of Cleaner Production* 251: 119550.

Herbert S and Wurzel A (2003) The effects of climate change on the vegetation of central European cities. *Urban Habitats* 1.

Ivanovsky L, Khryashchev V, Pavlov V, et al (2019) *Building detection on aerial images using U-net neural networks*. In: Conference of Open Innovations Association (FRUCT), Istanbul, Türkiye, 8-12 April 2019. IEEE, 116–122.

Janhäll S (2015) Review on urban vegetation and particle air pollution–deposition and dispersion. *Atmospheric Environment* 105: 130–137.

Jiang Z, Cheng H, Zhang P, et al. (2021) Influence of urban morphological parameters on the distribution and diffusion of air pollutants: A case study in China. *Journal of Environmental Sciences* 105: 163–172.

Jin K, Wang F and Li P (2018) Responses of vegetation cover to environmental change in large cities of China. *Sustainability* 10(1): 270.

Johnson WB, Ludwig FL, Dabberdt WF, et al. (1973) An urban diffusion simulation model for carbon monoxide. *Journal of the Air Pollution Control Association* 23(6): 490–498.

Khan SH, He X, Porikli F, et al. (2017) Forest change detection in incomplete satellite images with deep neural networks. *IEEE Transactions on Geoscience and Remote Sensing* 55(9): 5407–5423.

Lin W, Ting Y, Chang X, et al. (2015) Calculating cooling extents of green parks using remote sensing: Method and test. *Landscape and Urban Planning* 134: 66–75.

Lugg GA (1968) Diffusion coefficients of some organic and other vapors in air. *Analytical Chemistry* 40(7): 1072–1077.

Maimaitiyiming M, Abduwasit G, Tiyip T, et al. (2014) Effects of green space spatial pattern on land surface temperature: Implications for sustainable urban planning and climate change adaptation. *ISPRS Journal of Photogrammetry and Remote Sensing* 89: 59–66.

Majda AJ and Kramer PR (1999) Simplified models for turbulent diffusion: theory, numerical modelling, and physical phenomena. *Physics Reports* 314(4–5): 237–574.

Mapbox. Mapbox. https://www.mapbox.com/, 2010 (accessed 01 July 2020).
Nesbitt L, Meitner MJ, Girling C, et al. (2019) Who has access to urban vegetation? a spatial analysis of distributional green equity in 10 US cities. *Landscape and Urban Planning* 181: 51–79.
OpenStreetMap. Tileset. https://wiki.openstreetmap.org/wiki/Slippy_map_tilenames/, 2018 (accessed 01 July 2020).
Ovaskainen O (2002) Long-term persistence of species and the Sloss problem. *Journal of Theoretical Biology* 218(4): 419–433.
Ren Z, Zheng H, He X, et al. (2015) Estimation of the relationship between urban vegetation configuration and land surface temperature with remote sensing. *Journal of the Indian Society of Remote Sensing* 43(1): 89–100.
Roberts PJW. and Webster DR (2002) Turbulent diffusion.
Robitu M, Musy M, Inard C, et al. (2006) Modeling the influence of vegetation and water pond on urban microclimate. *Solar energy* 80(4): 435–447.
Ronneberger O, Fischer P and Brox T (2015) U-net: Convolutional networks for biomedical image segmentation. In: *International Conference on Medical image computing and computer-assisted intervention*, Munich, Germany, 5th to 9th October 2015. Springer, 234–241.
Rusche K, Reimer M and Stichmann R (2019) Mapping and assessing green infrastructure connectivity in European city regions. *Sustainability* 11(6): 1819.
Santiago S and Pascual-Hortal L (2007) A new habitat availability index to integrate connectivity in landscape conservation planning: comparison with existing indices and application to a case study. *Landscape and Urban Planning* 83(2–3): 91–103.
Siti NKBA, Shiraishi S, Inoshita T, et al. (2016) Analysis of satellite images for disaster detection. 2016 IEEE International Geoscience and Remote Sensing Symposium (IGARSS), 10–15 July 2016. IEEE, 5189–5192.
Supervisely. Supervisely. https://supervise.ly/, 2018 (accessed 01 July 2020).
Takebayashi Hideki (2017) Influence of urban green area on air temperature of surrounding built-up area. *Climate* 5(3): 60.
Thomas M (1999) *Cover. Elements of Information Theory*. Hoboke, NJ: John Wiley & Sons.
Tong X, Brandt M, Yue Y, et al. (2018) Increased vegetation growth and carbon stock in China karst via ecological engineering. *Nature Sustainability* 1(1): 44–50.
Wang JH (1965) Self-diffusion coefficients of water. *The Journal of Physical Chemistry* 69(12): 4412–4412.
Warhaft Z (2000) Passive scalars in turbulent flows. *Annual Review of Fluid Mechanics* 32(1): 203–240.
Xing Y and Peter B (2019) Role of vegetation in deposition and dispersion of air pollution in urban parks. *Atmospheric Environment* 201: 73–83.
Yin R, Xing W, Wei X, et al. (2011) Relationship between vegetation carbon storage and urbanization: a case study of Xiamen, China. *Forest Ecology and Management* 261(7): 1214–1223.
Zanjirani Farahani R, SteadieSeifi M and Asgari N (2010) Multiple criteria facility location problems: A survey. *Applied Mathematical Modelling* 34(7): 1689–1709.
Zhang X, Zhong T, Feng X, et al. (2009) Estimation of the relationship between vegetation patches and urban land surface temperature with remote sensing. *International Journal of Remote Sensing* 30(8): 2105–2118.

Author Biographies

Eric K Tokuda is a post-doctoral fellow at the Institute of Physics at the University of SÃ£o Paulo (USP). He has previously finished his PhD at the Computer Science Department at the Institute of Mathematics and Statistics at the same university. His main interests include computer vision and complex networks.

Florence AS Shibata has a bachelor's degree in Computer Science at University of SÃ£o Paulo (USP) and is currently finishing a master's degree course in Computer Science at USP. Areas of expertise and interest include: image processing, computer vision, data science, machine learning, deep learning.

Henrique Ferraz de Arruda is post-doc in the Instutute of Physics of SÃ£o Carlos - USP, Brazil. He holds a Ph.D. in Computer Science and Computational Mathematics from the Institute of Mathematics and Computer Sciences - USP, Brazil. Among his most outstanding achievements, he was awarded the best Ph.D. thesis in Brazil, CAPES Thesis Award Edition - 2020, in computer science. His primary research interests include models of real-world systems through network science, data analysis, natural language processing, and machine learning.

Guilherme Schimidt Domingues holds a BA in Computational Physics from the Institute of Physics of SÃ£o Carlos at the University of SÃ£o Paulo (IFSC-USP, Brazil), where he participated in two scientific initiations working with Network Science applied to models of urban cities and which yielded the publication of an article entitled Topological characterization of world cities (2018). He completed his master's degree in Computational Physics in 2020, in the area of Network Science, also from the same Institute, where he worked with optimization of network topology through link addition. Currently enrolled in the PhD course in Computational Physics by the same Institute.

Dr. Cesar H Comin received his Ph.D. in Computational Physics in 2016 from the University of SÃ£o Paulo and completed a postdoctoral fellowship at the same university in 2017. He is currently an Assistant Professor at the Federal University of SÃ£o Carlos, SÃ£o Paulo, Brazil. His main areas of research are Digital Image Processing, Complex Networks, and Machine Learning. Research topics include the automated grading of prostate cancer on histopathology images, development of semi-supervised approaches for 3D image segmentation, developing new tools for measuring the tortuosity of tubular structures and the definition of graph-theoretical approaches for characterizing biological and urban systems.

Luciano da F. Costa has a BSc in Electronic Eng. (USP), MSc in Applied Physics (USP), and PhD in Electronic Eng. (King's College London). He is a full Professor at the SÃ£o Carlos Institute of Physics, USP, Brazil. His areas of interest include complex systems, pattern recognition, image analysis, and analog and digital electronics.

Roberto M Cesar-Jr is a Full-Professor in the Department of Computer Science - IME - USP working in the Data Science Research Group. He served as the Director of the eScience Research Center at USP and as the head of the Computer Science Department. He was member of the Image and Vision Computing and the Signal, Image and Video Processing editorial boards, chair and invited speaker of conferences and workshops (Sibgrapi 2003, CIARP 2010, Sibgrapi 2011; SHAPES 2.0 - 2012, eSon - IEEE eScience 2013, IEEE eScience 2014). He has experience in computer science, with emphasis on computer vision, machine learning and artificial intelligence.